Study on the Flow in Idealized Hybrid Rocket Motor using Large Eddy Simulation Technique

C. Lee and Y. Na***

**Dept. of Aerospace Engineering, Konkuk University*

Gwangjin-gu, Hwayang-dong 1, Seoul 143-701, Korea

***Corresponding Author, Dept. of Mechanical Engineering,*

Konkuk University, Gwangjin-gu, Hwayang-dong 1, Seoul 143-701, Korea

Abstract

Motivated by recent experimental observation of the noticeable feature of roughness on the fuel grain surface in the hybrid rocket combustion chamber, a simplified model rocket motor was investigated through a large eddy simulation (LES) technique to understand how the turbulent structures are modified in the vicinity of fuel surface. It was found that the structural feature has been altered by the application of wall injection, which is reminiscent of patterns of the isolated roughness observed in the experiment. This abrupt change of flow characteristics is accompanied by the rapid movement of coherent structures away from the wall.

1. Introduction

Hybrid rocket is attracting much attention these days due to its well-known safety and low development cost. However, in order to be effectively applied in a wide range of propulsion systems, its low density specific impulse needs to be drastically improved. Thus, currently much effort is being made towards devising a better of way increasing the regression rate of a hybrid fuel. Vortex type rocket is one of those examples which significantly increase the residence time by manipulating the fluid dynamical aspect of the oxidizer flow.

Combustion process inside the hybrid motor, characterized by the diffusion flame, is extremely difficult to analyze due to its non-linear interaction between the main flow of oxidizer and vaporization process of the fuel. In addition to this difficulty, the complicated coupling between the pressure and density fluctuations makes any attempt of realistic analysis almost impossible. Thus, many researchers in this area naturally resort to the measurement technique in the absence of confidence for the realistic numerical simulation at reasonable cost. Admitting that the general numerical prediction tool is still far from being satisfactory even with the current computer resources, any attempt of large eddy simulation (LES) even in the simplified situation can be of great importance since the large scale turbulent structures which basically govern the transport phenomenon can be captured correctly. This could be a main advantage of LES over the historically popular RANS type simulations.

Some of recent experimental results reported to the literature [1, 2] have clearly indicated that the enhanced regression rate constantly left the isolated surface roughness pattern on the fuel surface. These circular or elliptic isolated patterns probably resulted from an incomplete combustion process but, interestingly enough, the same behaviour persists in the case of excessive supply of oxidizer over the O/F ratio [1]. The origin of these noticeable features is not still well understood at the moment but is just conjectured to be attributed to the modification of turbulent structures by the regression process. Like mentioned earlier, obtaining a clue for the reason of getting this surface pattern is very important to understand the physics of the regression process but the phenomenon is not still well explained. In the present study, LES technique was adopted to compromise between the accuracy and the cost with a hope that detailed flow field information even in simplified model geometry can provide the physical insight.

In order to make the analysis realistic, the Reynolds number was set to that of the experiment [1], which, in fact, severely puts the restriction on the resolution requirement. Thus, up to 51 million grid points were used for the present numerical simulation in order to resolve the relevant turbulent scales. To create a better focus on the near-wall turbulent flow with an acceptable cost, model rocket motor was idealized by the simple channel and the chemical reaction was not considered. However, the temperature was assumed to be a passive scalar with Prandtl number being 1.

In the next section, numerical methodology will be described in detail followed by the various instantaneous and statistical results.

2. Numerical methodology

One of the most popular LES model is, perhaps, the dynamic Smagorinsky model (DSM). This model has been successfully applied to a various class of flows for the past 15 years. Even with the proven validity, its excessive dissipative nature causes a series of further modification of the model. One of such successful efforts is so-called dynamic mixed model (DMM) developed by Zang et al. [3]. This model, which has also been tested for a variety of flows, is known for a better performance than its predecessor, DSM. Details on the methodology of DMM and its straightforward extension to the calculation of passive scalar will be found in Na [4].

2.1 Governing equation for LES

Considering the fact that the flow velocity inside the hybrid motor remains relatively low compared to the sonic velocity in the accompanying experiment, the flow is assumed to be incompressible. Thus, the filtered transport equation for the passive scalar in addition to continuity and momentum equations are described as follow:

$$\frac{\partial \overline{u_i}}{\partial x_i} = 0 \tag{1}$$

$$\frac{\partial \overline{u_i}}{\partial t} + \frac{\partial}{\partial x_j}(\overline{u_i}\,\overline{u_j}) = -\frac{\partial \overline{p}}{\partial x_i} + \frac{\partial}{\partial x_j}(2\nu \overline{S_{ij}} - \tau_{ij}) \tag{2}$$

$$\frac{\partial \overline{T}}{\partial t} + \frac{\partial}{\partial x_j}(\overline{u_j}\,\overline{T}) = \frac{\partial}{\partial x_j}(\alpha \frac{\partial \overline{T}}{\partial x_j} - q_j) \tag{3}$$

Here, the overbar denotes the grid filtering operation. In order to close the governing equations mathematically, LES models for the following residual stress tensor τ_{ij} and the residual heat flux vector q_j should be provided.

$$\tau_{ij} = \overline{u_i u_j} - \overline{u_i}\,\overline{u_j} \ , \ q_j = \overline{T u_j} - \overline{T}\,\overline{u_j} \tag{4}$$

Since the DMM of Zang et al. [3] was adopted in the present study, the following procedure was incoporated for calculation of the turbulent velocity field with a box filter in physical space.

$$\tau_{ij} - \frac{\delta_{ij}}{3}\tau_{kk} = -2\nu_t \overline{S_{ij}} + (L^m_{ij} - \frac{\delta_{ij}}{3} L^m_{kk}) \tag{5}$$

$$\nu_t = C_s \overline{\Delta}^2 \overline{S} \ , \ L^m_{ij} = \overline{\overline{u_i}\,\overline{u_j}} - \overline{\overline{u_i}}\,\overline{\overline{u_j}} \tag{6}$$

Modified Leonard term is explicitly calculated using the filtered flow field and the turbulent viscosity ν_t is determined dynamically through the following steps using the test filtering operation denoted by tilde.

$$C_S = \frac{1}{2\overline{\Delta}^2} \frac{M_{ij}(L_{ij} - H_{ij})}{M_{kl} M_{kl}} \tag{7}$$

$$M_{ij} = \left[\widetilde{\overline{S}\,\overline{S}_{ij}} - (\tilde{\overline{\Delta}} / \overline{\Delta}) \tilde{\overline{S}}\,\tilde{\overline{S}}_{ij} \right], \quad L_{ij} = \widetilde{\overline{u}_i \overline{u}_j} - \tilde{\overline{u}}_i \tilde{\overline{u}}_j, \quad H_{ij} = \widetilde{\overline{\overline{u}}_i \overline{\overline{u}}_j} - \tilde{\overline{\overline{u}}}_i \tilde{\overline{\overline{u}}}_j \tag{8}$$

The procedure of DMM for getting the velocity field can be extended to the passive scalar in a similar manner for evaluating the residual heat flux vector q_j. As was done for the residual stress tensor, heat flux vector consists of two terms and the turbulent diffusivity is obtained dynamically as explained in the following.

$$q_j = -\alpha_t \frac{\partial \overline{T}}{\partial x_j} + F_j^m \tag{9}$$

$$\alpha_t = C_T \overline{\Delta}^2 \overline{S}, \quad F_j^m = \overline{\overline{T} u_j} - \overline{\overline{T}}\,\overline{\overline{u}}_j \tag{10}$$

$$C_T = \frac{1}{\overline{\Delta}^2} \frac{(F_k - G_k) H_k}{H_k H_k} \tag{11}$$

$$F_k = \widetilde{\overline{T}\,\overline{u}_k} - \tilde{\overline{T}}\,\tilde{\overline{u}}_k, \quad G_k = \widetilde{\overline{\overline{T}}\,\overline{\overline{u}}_k} - \tilde{\overline{\overline{T}}}\,\tilde{\overline{\overline{u}}}_k, \quad H_k = \widetilde{\overline{S} \frac{\partial \overline{T}}{\partial x_k}} - (\tilde{\overline{\Delta}} / \overline{\Delta})^2 \tilde{\overline{S}} \frac{\partial \tilde{\overline{T}}}{\partial x_k} \tag{12}$$

Governing equations (1)-(3) are integrated in time using a semi-implicit procedure (Na [5]). The convective term is treated by the 3rd order Runge-Kutta method and the viscous term is integrated by the 2nd order Crank-Nicolson scheme. All the spatial derivatives were conducted by the 2nd order central difference scheme except for the convective term of Eq. (3). Noting the fact that the central difference scheme for the convective term of passive scalar equation suffers from the numerical instability, this problem was effectively suppressed by the use of popular QUICK scheme [6].

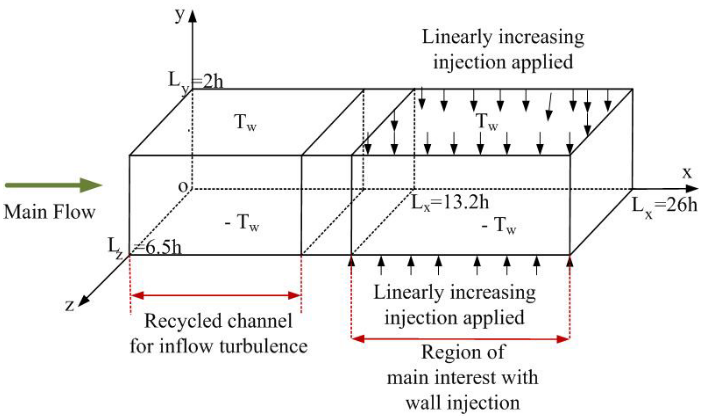

Figure 1: Schematic of numerical domain

2.2 Computational geometry

Numerical domain is shown in Fig. 1. As was explained earlier, the model rocket motor was idealized by the simple channel and the regression process is approximated by the injection of the fluid at the wall. Since the main scope of the present work is to examine the interaction of main and the injected flows, which basically occur in the near-wall boundary layer, neglecting the curvature effect is not believed to deteriorate the validity of the present numerical result significantly.

In order to supply the physically realistic turbulence to the region of interest with wall injection, the flow is continuously recycled in the channel placed in front of the domain so that it allows the spatial room for developing realistic turbulence. It turns out that this devise of flow configuration generates physically acceptable coherent structures making the present analysis very realistic from the point of flow dynamics.

Reynolds number based on inlet bulk velocity and the half channel height was set to 22,500, which is very close to that of the physical experiment and the Prandtl number was set to 1. Relatively high Reynolds number chosen here requires a huge expenditure due to the presence of very small scales. Thus, a series of computations was conducted with different resolutions before we settled down with 513x193x513 grid system (approximately 51 million grids). All the results shown here are based on this grid system.

2.3 Boundary condition

No-slip boundary condition was assumed along the wall except in the second half of the channel where injection is applied. The magnitude of the injected vertical velocity is varying linearly from the 1% to 3% as was seen in the experiment. Constant temperatures were maintained along the walls with the lower wall at higher temperature. Since the temperature was assumed to be a passive scalar, having a higher temperature at lower wall does not cause the density change.

Periodic boundary condition was imposed in the spanwise direction and the convective boundary condition was specified at the exit in order to allow turbulence structures to leave the domain with minimal distortion.

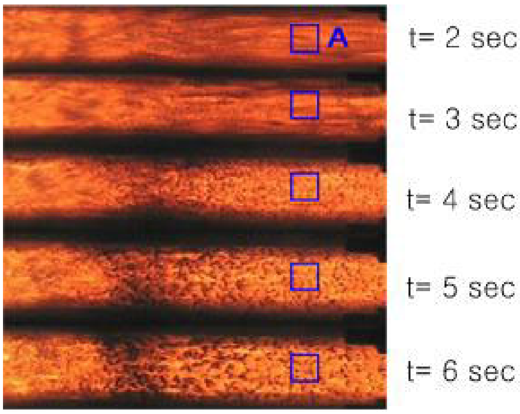

Figure 2: Sequential visualization of combustion process with PMMA

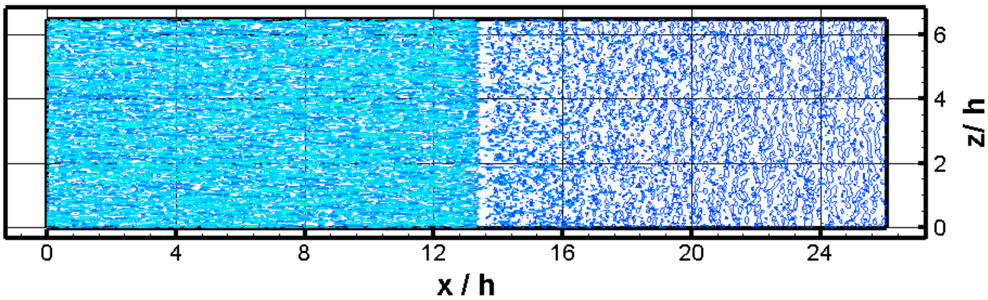

(a) y/h=0.0001

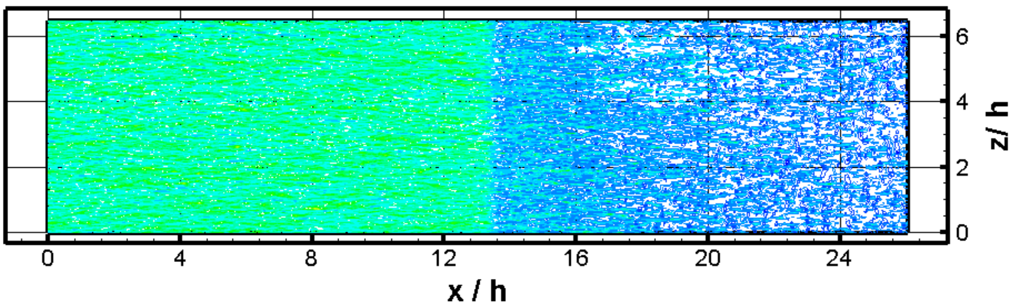

(b) y/h=0.05

Figure 3: Instantaneous snapshots of streamwise velocity at two different (x-z) planes

3. Results

Fig. 2 shows the sequential progress of combustion process with equal time interval. PMMA was used as a fuel in a cylindrical shape. At early stage of combustion (*i.e.* up to 3 seconds), streaky patterns reminiscent of typical turbulent structures are displayed. They are much more elongated in the streamwise direction. Later, however, isolated circular patterns appear and grow as the combustion progresses. The stage after the initiation of combustion process is characterized by the increasing regression rate at the wall. As the regression process or wall blowing becomes increases, this injected momentum starts to interact with the main flow. Thus, the change of observed pattern can be attributed to the disturbance incurred by the injection. Considering the fact that different set of experimental configuration with inlet swirl investigated in our laboratory also produces the similar behaviour suggests that the sudden change of visualized features is more likely related to the structural change of coherent structures.

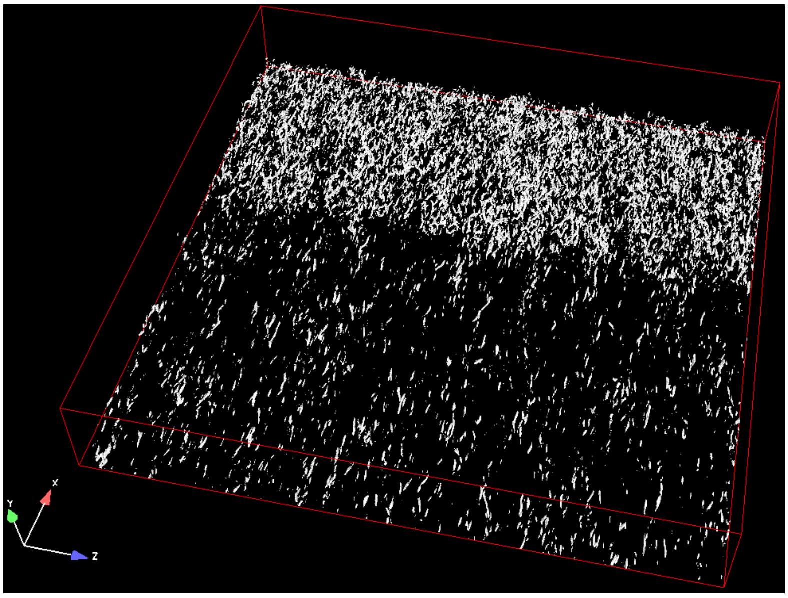

Figure 4: Iso-surface of coherent structures in a region where wall injection begins

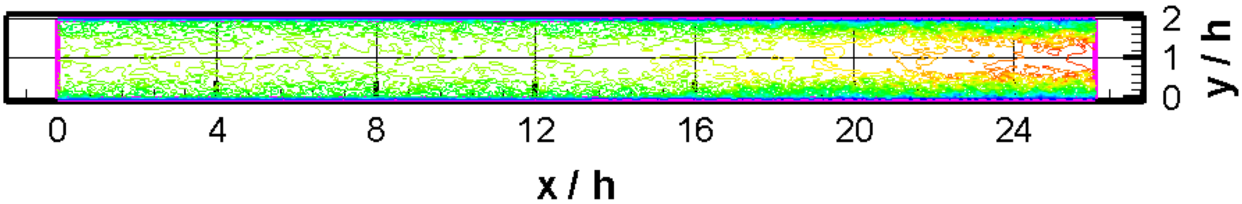

(a) streamwise velocity

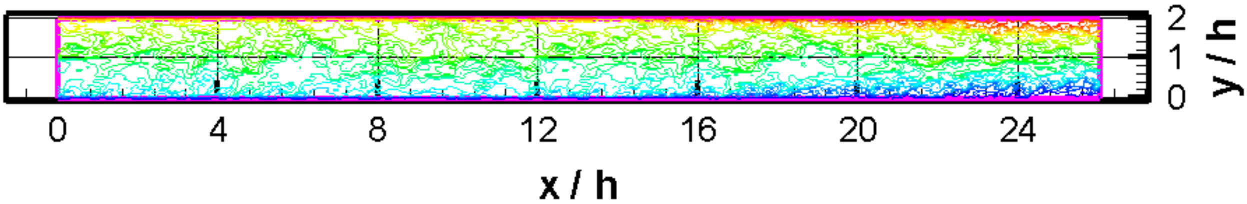

(b) temperature

Figure 5: Snapshots of instantaneous streamwise velocity and temperature at mid (x-y) plane

Contours of instantaneous streamwise velocity in the plane close to the wall (Fig. 3a) clearly show that the structural feature has been altered by the application of wall injection, which is, again, reminiscent of patterns of the isolated roughness found in the experiment (Fig. 2). This abrupt change of flow characteristics is accompanied by the rapid movement of coherent structures away from the wall. Using a method of vortex identification (eigenvalues of velocity gradient tensor), visualization of coherent structures was made. A close examination of iso-contours of coherent structures displayed in Fig. 4 reveals that the streaky structures generated upstream of wall injection (they tend to be aligned more or less in the main flow direction) are displaced away from the wall, leaving more isolated circular contours on the surface as a footprint. In addition to this displacement, the shear layer resulting from the interaction of main flow with the wall injection contributes to the abundant supply of coherent structures also seen in Fig. 3b.

Fig. 5 shows how the hydrodynamic and thermal boundary layers react to the wall injection. Flow experiences strongly acceleration due to the addition of mass through the wall and this results in strong inhomogeneity in the streamwise direction in the region of x/h>13.2. Also farther displacement of thermal boundary layer away from the wall is evident in this figure. Since the temperature field was assumed as a passive scalar, this indicates that diffusions of momentum and passive scalar are occurring at different rates. Mean streamwise velocity and temperature profiles at several representative streamwise locations (Fig. 6) also imply that the friction temperature, which is the relevant to the ratio of velocity gradient and temperature gradient at the wall, becomes smaller in the region of wall injection. This sudden decrease of temperature gradient at the wall will eventually suppress the conduction heat transfer to the surface, resulting in the suppression of regression rate.

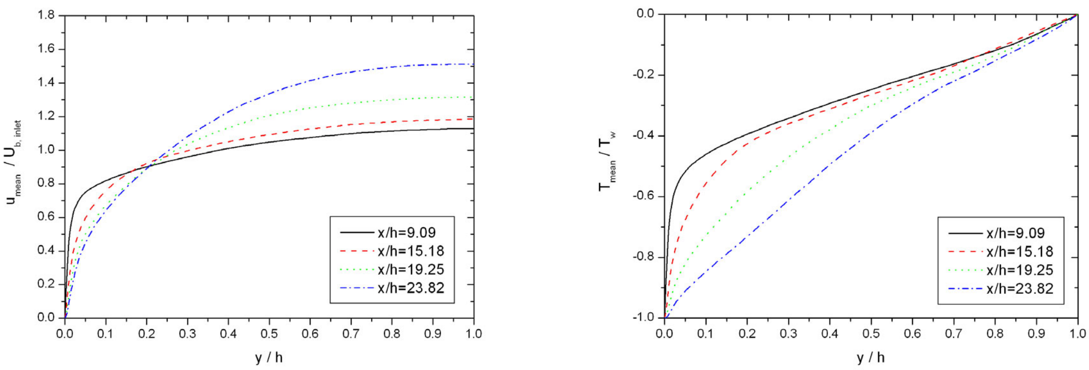

(a) mean streamwise velocity (b) mean temperature

Figure 6: Mean profiles at several locations

One of the main interests is the behaviour of turbulence activity away from the wall. Fig. 7 shows the turbulent stress and heat flux in the wall normal direction at several locations. Due to the interaction of main oxidizer flow with the wall blowing, a very strong shear layer develops away from the wall. In this shear layer, coherent structures multiply very rapidly as shown in Fig. 4 and cause a sudden increase of turbulent heat flux in the vertical direction as well as Reynolds shear stress. It is noted that the location of maximum heat flux is displaced further away from the wall than that of Reynolds shear stress. This behaviour is consistent with the findings shown in both the instantaneous and statistical results given in Figs. 5 and 6.

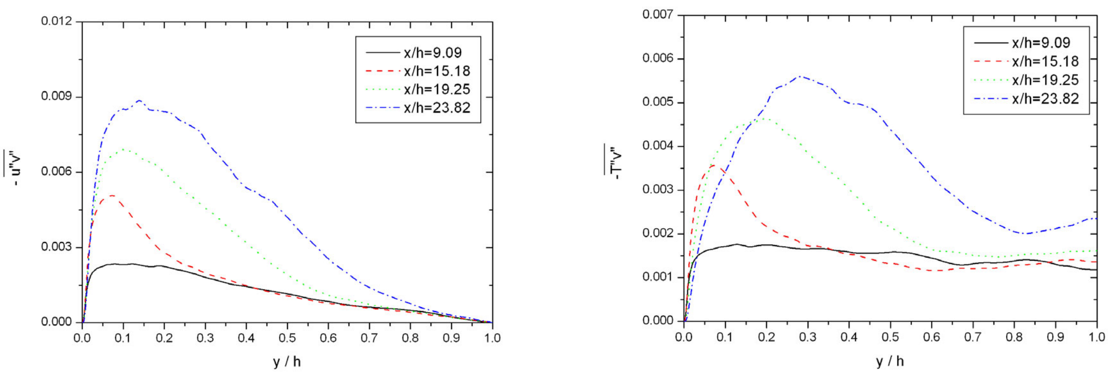

(a) mean streamwise velocity (b) mean temperature

Figure 7: Turbulent transport statistics at several locations

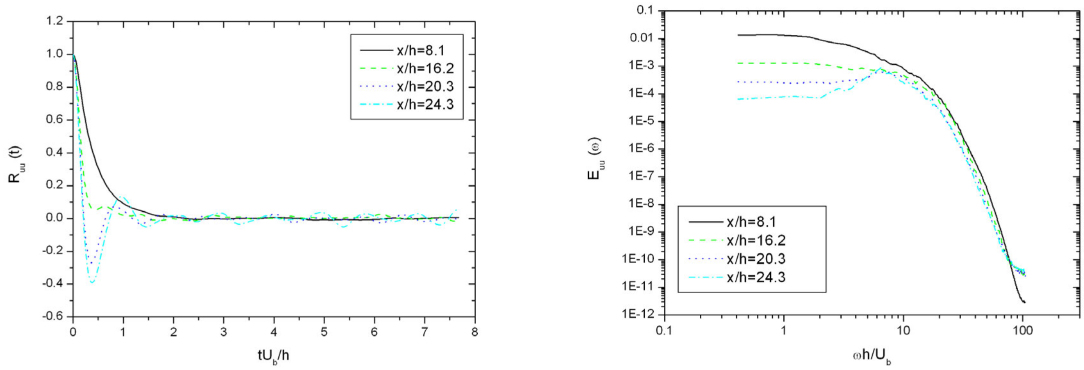

(a) auto-correlation (b) frequency spectra

Figure 8: Time characteristics of streamwise velocity in the vicinity of wall

Finally, the time-scale of the flow in the vicinity of the wall was pursued by inspecting the frequency spectra and auto correlation of streamwise velocity (Fig. 8). Note that, in the presence of wall blowing, very large negative excursion develops in the auto correlation. For reference, it should be noted that the location of x/h=8.1 corresponds to the simple change without wall injection. It is obvious that this unexpected feature reflects the complicated change of structural feature of coherent structures. If Taylor's hypothesis is used here, the behaviour in the time direction can be converted into that in the streamwise direction. The presence of large negative correlation would mean that near-wall streaky structures are not as long as in upstream but they break down into several pieces due to the action of injection. This behaviour is consistent with the appearance of isolated circular patterns in Fig. 3a. Since the vortical structures are too crowded in Fig. 4, it is not easy to measure the change of size of those structures but a more careful investigation is being conducted.

Frequency spectra also display the presence of very distinctive peak near non-dimensional frequency near 6 after the application of wall injection. This characteristic Strouhal number is much greater than that of typical vortex shedding flow configuration such as in backward facing step. Unfortunately, we are unable to find the origin for this behaviour at the moment. Complete explanation will require more flow field information and this constitutes our future study.

4. Summary

Large eddy simulation was performed in an idealized model rocket motor with an objective of understanding the origin of isolated surface roughness patterns seen in several recent experiments. In particular, emphasis was put on evolution of near-wall turbulent structures in the presence of wall injection. Dynamic procedure combined with dynamic mixed model was incorporated and up to 51 million grid points were used in order to capture the essential features of 3-D, unsteady turbulent fields.

The flow is characterized by the non-negligible streamwise inhomogeneity due to the disturbance generated by injected flows at the wall. Several turbulent statistics and correlations indicate that the wall injection drastically change the characteristics of the near-wall turbulence. Contours of instantaneous streamwise velocity in the plane close to the wall clearly show that the structural feature has been significantly altered by the application of wall injection, which is reminiscent of the isolated roughness patterns found in several experiments. This abrupt change of flow characteristics is accompanied by the rapid movement of coherent structures away from the wall. Close examination of iso-contours of coherent structures reveal that the streaky structures generated upstream of wall injection are displaced away from the wall, leaving more isolated circular contours on the fuel surface. Thus, the sequential change of patterns observed in the experiment (Fig. 2) is believed to be strongly related to the change in kinematic configuration of near-wall structures. Of course, the present study assumes the cold flow without the effect of significant density variation and this would limit the accuracy of our conjecture but, overall flow feature is not likely to be changed even in the real combustion process. However, auto-correlation and the frequency spectra still leave unanswered questions and our next future work consists of the more rigorous investigation on these issues.

References.

[1] Koo, W. and Lee, C. The Combustion Characteristics of Oxidizer Flow Change in Hybrid Rocket. Proceedings of the 2007 Korean Society of Propulsion Engineers Spring Conference, Korea, April 2007.

[2] Evans, B., Favorito, N. A. and Kuo, K. K. Oxidizer-Type and Aluminum-Particle Addition Effects on Solid Fuel Burning Behaviour. AIAA Paper 2006-4676, 42nd AIAA/ASME/SAE/AEE Joint Propulsion Conference & Exhibit, U.S.A. July 2006.

[3] Zang, W., Street, R. L. and Koseff, J. R. A Dynamic Mixed Subgrid-scale Model and its Application to Turbulent Recirculating Flows. Phys. Fluids, 12: 3186-3196, 1993.

[4] Na, Y. On the Large Eddy Simulation of Scalar Transport with Prandtl Number up to 10 Using Dynamic Mixed Model, *Journal of Mechanical Science and Technology*, 19:913-923, 2005.

[5] Na, Y. Direct Numerical Simulation of Turbulent Scalar Field in a Channel with Wall Injection. *Numerical Heat Transfer A*, 47:165-181, 2005.

[6] Leonard, B. P. A Stable and Accurate Convective Modelling Procedure Based on Quadratic Upstream Interpolation. *Comput. Methods Appl. Mech. Eng*., 19:59-98, 1979.

This page has been purposedly left blank